

This is the peer reviewed version of the following article:

Basin-scale analysis of the geomorphic effectiveness of flash floods: A study in the northern Apennines (Italy) / Scorpio, V.; Crema, Silvia; Marra, F.; Righini, M.; Ciccicarese, G.; Borga, M.; Cavalli, M.; Corsini, A.; Marchi, L.; Surian, N.; Comiti, F.. - In: SCIENCE OF THE TOTAL ENVIRONMENT. - ISSN 0048-9697. - 640-641:(2018), pp. 337-351. [10.1016/j.scitotenv.2018.05.252]

*Terms of use:*

The terms and conditions for the reuse of this version of the manuscript are specified in the publishing policy. For all terms of use and more information see the publisher's website.

18/12/2025 18:56



# Basin-scale analysis of the geomorphic effectiveness of flash floods: A study in the northern Apennines (Italy)

V. Scorpio<sup>a,\*</sup>, S. Crema<sup>b,c</sup>, F. Marra<sup>d</sup>, M. Righini<sup>e</sup>, G. Ciccacese<sup>f</sup>, M. Borga<sup>b</sup>, M. Cavalli<sup>c</sup>, A. Corsini<sup>f</sup>, L. Marchi<sup>c</sup>, N. Surian<sup>e</sup>, F. Comiti<sup>a</sup>

<sup>a</sup> Faculty of Science and Technology, Free University of Bozen-Bolzano, Bolzano, Italy

<sup>b</sup> Department of Land, Environment, Agriculture and Forestry, University of Padova, Padova, Italy

<sup>c</sup> Research Institute for Geo-hydrological Protection, National Research Council (CNR IRPI), Padova, Italy

<sup>d</sup> Institute of Earth Sciences, The Hebrew University of Jerusalem, Jerusalem, Israel

<sup>e</sup> Department of Geosciences, University of Padova, Padova, Italy

<sup>f</sup> Department of Chemical and Geological Sciences, University of Modena and Reggio Emilia, Modena, Italy

## ARTICLE INFO

### Article history:

Received 30 December 2017

Received in revised form 18 May 2018

Accepted 21 May 2018

Available online xxx

### Keywords:

Channel widening  
Bed level changes  
Stream power  
Channel confinement  
Flash flood  
Flood geomorphic hazard

## ABSTRACT

Large floods may produce remarkable channel changes, which determine damages and casualties in inhabited areas. However, our knowledge of such processes remains poor, as is our capability to predict them. This study analyses the geomorphic response of the Nure River (northern Italy) and nine tributaries to a high-magnitude flood that occurred in September 2015. The adopted multi-disciplinary approach encompassed: (i) hydrological and hydraulic analysis; (ii) analysis of sediment delivery to the stream network by means of landslides mapping; (iii) assessment of morphological modifications of the channels, including both channel width and bed elevation changes.

The spatial distribution of rainfall showed that the largest rainfall amounts occur in the upper portions of the catchment, with cumulative rainfall reaching 300 mm in 12 h, and recurrence intervals exceeding 100–150 years. The unit peak discharge ranged between 5.2 and 25 m<sup>3</sup> s<sup>-1</sup> km<sup>-2</sup>. Channel widening was the most evident effect. In the tributaries, the ratio between post-flood and pre-flood channel width averaged 3.3, with a maximum approaching 20. Widening was associated with channel aggradation up to 1.5 m and removal of riparian vegetation. New islands formed due to the fragmentation of the former floodplain. In the Nure River, the average width ratio was 1.7, and here widening occurred mainly at the expenses of islands. Bed level dynamics in the Nure were varied, including aggradation, incision, and overall stability. The flood geomorphic effectiveness was more pronounced in the middle-higher portions of the basin. Planimetric and elevation changes were well correlated. Regression analysis of the relationship between widening and morphological/ hydraulic controlling factors indicated that unit stream power and confinement index were the most relevant variables.

The study provides useful insights for river management, especially with regard to the proportion of the valley floor subject to erosion and/or deposition during large events.

© 2017.

## 1. Introduction

Floods are among the most relevant natural events causing geomorphological channel changes and fluvial landscape development (Hooke, 2015; Stoffel et al., 2016). Extreme floods induce physical impacts on the channels and the valley bottoms, such as widening (Krapesch et al., 2011), changes in bed level, channel position and

patterns, extensive bar formation, erosion and construction of islands (Belletti et al., 2014), meander migration, avulsions, bank erosion (Grove et al., 2013), and floodplain accretion (Hauer and Habersack, 2009). The geomorphic effectiveness of floods has been widely studied worldwide (Wolman and Gerson, 1978; Hooke, 2015; Surian et al., 2016) but, while effects on channel width are documented for several floods, fewer studies describe the vertical changes on channels and floodplains. Generally, deposition occurs on bars and floodplains (Hooke and Mant, 2000; Magilligan et al., 1998; Hooke, 2016). Aggradation is very common immediately downstream of tributary junctions (Sloan et al., 2001; Dean and Schmidt, 2013), where the channel bed presents lower slope (Dean and Schmidt, 2013), or in areas where the valley widens (Cenderelli and Wohl, 2003; Hauer and Habersack, 2009) and channels are unconfined (Thompson and Croke, 2013). Channels experience bed incision (Sloan et al., 2001),

\* Corresponding author at: Faculty of Science and Technology, Free University of Bozen-Bolzano, Piazza Università 5, 39100 Bolzano, Italy.

Email addresses: [Vittoria.Scorpio@unibz.it](mailto:Vittoria.Scorpio@unibz.it) (V. Scorpio); [stefano.crema@irpi.cnr.it](mailto:stefano.crema@irpi.cnr.it) (S. Crema); [marra.francesco@mail.huji.ac.il](mailto:marra.francesco@mail.huji.ac.il) (F. Marra); [margherita.righini@studenti.unipd.it](mailto:margherita.righini@studenti.unipd.it) (M. Righini); [giuseppe.ciccacese@unimore.it](mailto:giuseppe.ciccacese@unimore.it) (G. Ciccacese); [marco.borga@unipd.it](mailto:marco.borga@unipd.it) (M. Borga); [marco.cavalli@irpi.cnr.it](mailto:marco.cavalli@irpi.cnr.it) (M. Cavalli); [alessandro.corsini@unimore.it](mailto:alessandro.corsini@unimore.it) (A. Corsini); [lorenzo.marchi@cnr.it](mailto:lorenzo.marchi@cnr.it) (L. Marchi); [nicola.surian@unipd.it](mailto:nicola.surian@unipd.it) (N. Surian); [Francesco.Comiti@unibz.it](mailto:Francesco.Comiti@unibz.it) (F. Comiti)

especially with floods with low sediment load (Dean and Schmidt, 2013) or downstream of sediment retention sites, such as dams (Hooke and Mant, 2000). Erosion has been found to be most common in narrow, steep reaches where the channel is confined (Cenderelli and Wohl, 2003; Thompson and Croke, 2013).

Floods also control island patterns (Belletti et al., 2014). During floods, channels widen by removing woody vegetation from the islands. Floods, however, may also increase island number, as floodplains can be fragmented by the formation of new channels (Gurnell et al., 2001; Comiti et al., 2011; Belletti et al., 2014). Belletti et al. (2014) assert that flood return period is the main representative parameter for island development and spatial density. High magnitude floods increase island fragmentation, while low magnitude floods promote vegetation establishment and island coalescence. However, in the Tagliamento River, Surian et al. (2015) showed that significant vegetation erosion is determined also by relatively frequent floods, i.e. floods with a recurrence interval of about 1–2.5 years. On the other hand, extensive island erosion, in large braided rivers, seems to happen only for floods >10–20 years (Comiti et al., 2011; Surian et al., 2015).

Numerous studies have tried to determine the main factors controlling channel response to extreme flood events. Most of these studies focused on the influence of hydraulic variables, e.g. flow duration, magnitude, frequency, flow competence, flood power, duration of effective flows, sequence of events, unit stream power (Costa and O'Connor, 1995; Magilligan, 1992; Magilligan et al., 1998; Cenderelli and Wohl, 2003; Kale, 2007; Magilligan et al., 2015). However, some recent studies confirmed that hydraulic variables alone cannot fully explain the river response to floods (Heritage et al., 2004; Surian et al., 2016). In the light of these studies, they stress the important role of sediment supply, boundary conditions, flood flow patterns, valley orientation, antecedent channel conditions (Harvey, 2001; Cenderelli and Wohl, 2003; Hauer and Habersack, 2009; Dean and Schmidt, 2013; Buraas et al., 2014; Lallias-Tacon et al., 2017) and of artificial structures, e.g. embankments, weirs, rip-raps (Arnaud-Fassetta et al., 2005). In particular, valley confinement was found to be a key factor (Hauer and Habersack, 2009; Thompson and Croke, 2013; Surian et al., 2016; Righini et al., 2017). As shown by Thompson and Croke (2013), floods can cause only limited lateral erosion and widening in confined channels. Also, high stream power and narrow valley widths inhibit deposition processes (Hooke, 2016) and tend to favor channel incision. In unconfined channels, floods mainly cause channel widening and in-channel or floodplain aggradation.

Importantly, most of the previous studies were conducted on single rivers, without the possibility to analyze the spatial variability of the event magnitude in relation to the distribution of the rainfall event. On the other hand, Sloan et al. (2001) demonstrated that the effects on tributaries were markedly stronger compared to those observed in the main channel.

The present study analyses the geomorphic response of the Nure River basin, located in northern Italy, to a high-magnitude flood that occurred in September 2015. Approximately 38 km of the channel length of the Nure River and of 9 of its tributaries were analyzed. The specific aims of this study are: i) to quantify the channel morphological changes (width and bed elevation); ii) to quantify the response of vegetated surfaces (floodplains and islands); iii) to provide a basin-scale understanding of such morphological changes; iv) to assess the relative role of the different hydrological and morphological factors controlling the flood geomorphic effectiveness. Finally, some implications of our results for river corridor management, specifically in terms of the definition of flood hazard, are discussed.

## 2. Study area

The Nure River is located in the northern Apennines (northwestern Italy), and its catchment drains an area of 430 km<sup>2</sup>, elongated in the SW-NE direction (Fig. 1a). The Nure originates at about 1500 m a.s.l. and flows to the Po River after a total length of 75 km. The maximum elevation of the catchment is 1773 m a.s.l., the average is 800 m a.s.l. The basin is mainly composed of sedimentary rocks, especially sandstones and mudstones with some outcrops of volcanic rocks. Its physiography is mostly composed of mountains and hilly landscape (78% of the total area) (*sensu* Rinaldi et al., 2013). The Nure catchment is mostly forested in the mountainous and hilly sectors, while agricultural areas cover most of the lower part of the basin.

The mean annual precipitation is approximately 1150 mm; climate is temperate with cold winter and dry summer and most of the precipitation occurs during autumn and spring. Most of the Nure River is characterized by unconfined channel reaches, except for the upper part of the basin (above 850 m a.s.l.) where a narrow valley is present. From upstream to downstream, channel morphology shifts from sinuous to a sinuous with alternate bars (and/or wandering) to braided morphology, before returning to single-thread morphologies (sinuous and meandering) in the lower plain.

Several tributaries flow into the Nure River within its montane basin. These are mainly single-thread channels, except in their wider, most downstream reaches where sinuous with alternate bars or wandering patterns can establish.

The river network in Nure catchment features a very limited extent of artificial structures, except for the reaches crossing urban areas (e.g. Ferriere, Farini and Bettola) where the Nure is channelized and stabilized by grade-control structures. Before 2015, major flood events occurred in 1889 and 1910 (<http://www.adbpo.it/on-multi/ADBPO/Home/Pianificazione/Pianistralcioapprovati/PianostralcioperlAssettoIdrogeologicoPAI.html>).

On 14th September 2015, the Nure basin was affected by an extreme flood caused by a rainstorm that started in the morning of 13th September (9 am local time) and lasted approximately 24 h. The main burst of the storm started at around 5 pm local time and lasted approximately 12 h.

This study focuses on the Nure River basin upstream from the town of Ponte dell'Olio (drainage area of 337 km<sup>2</sup>). The analysis involved 37.8 km of the main channel within the montane and hilly portion of the catchment, as well as 9 tributaries over a total channel length of 33.6 km (Table 1 and Fig. 1a). These streams are characterized by coarse sediments (mainly gravel and cobbles), and highly variable lateral confinement, valley width, channel morphology and slope.

## 3. Materials and methods

The study was carried out by means of the multi-disciplinary approach proposed by Rinaldi et al. (2016). This methodological framework is based on field surveys, remote sensing analysis, and hydrological modelling and encompassed: (i) hydrological and hydraulic analysis of the flood event; (ii) analysis of sediment delivery to the channel network by means of landslides mapping; (iii) identification and estimation of wood recruitment, deposition and budgeting; (iv) analysis of fluvial processes and deposits; (v) assessment of morphological changes of channels and floodplains.

This study did not address explicitly large wood dynamics, as, for instance, in Lucia et al. (2015) or Steeb et al. (2017). During the

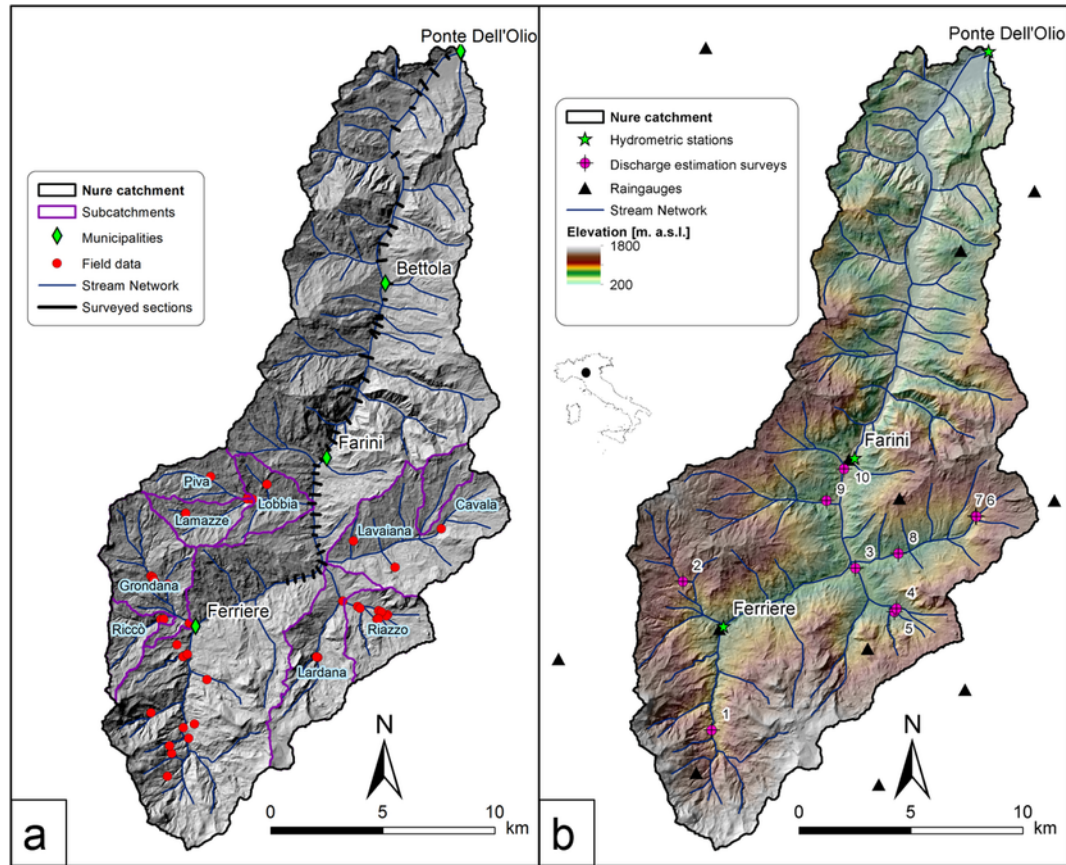


Fig. 1. Location map of the Nure Basin with studied channel segments (a); location of stream gauges, rain gauges and discharge estimations sites during post-flood surveys (b).

Table 1

River	Drainage area (km <sup>2</sup> )	Minimum/maximum basin elevation (m)	Channel length (km)	Average channel slope (%)
Nure	307	250–1773	37.8	1.76
Lobbia	22	452–1430	3.0	7.01
Lamazze	6	653–1402	2.0	9.78
Piva	8	653–1430	2.4	10.85
Grondana	23	650–1540	5.5	7.53
Riccó	6	653–1540	3.3	10.42
Lavaiana	32	520–1333	6.3	4.05
Cavala	5	629–1333	1.5	11.30
Lardana	30	487–1710	7.3	7.97
Riazzo	11	535–1160	2.3	7.03

Average slope evaluated for the channel length indicated in the table.

event, large wood transport was surely intense as extensive wooded areas (mostly islands and floodplains) were eroded (see later), but post-flood surveys revealed how only limited wood volumes were deposited or trapped by bridges and natural obstacles. Indeed, as also mentioned by Comiti et al. (2016), for this flood the vast majority of large wood traveled through the analyzed segment without being intercepted.

### 3.1. River network segmentation

As in Surian et al. (2016) and Righini et al. (2017), the studied channels (total of 72 km) were partitioned into sub-reaches applying the GIS-based approach proposed by Ferencevic and Ashmore

(2012). The subdivision into sub-reaches took into account the methodology proposed by Brierley and Fryirs (2005) and Rinaldi et al. (2013) that splits rivers in homogeneous reaches considering the occurrence of discontinuities as confluences of the most important tributaries, changes in lateral confinement, in valley orientation and slope, in channel width and planform pattern. The analysis was carried out by means of a 5-m resolution Digital Elevation Model (DEM) derived from a 1:5000-scale technical cartography (usually with a vertical accuracy ranging from  $\pm 0.5$  m to  $\pm 1$  m). A total of 175 sub-reaches were identified, their lengths range from a minimum of 110 m in the Grondana River to a maximum of 1370 m in the Nure River (Table 2). For each sub-reach, a number of morphological characterizing parameters were evaluated before and after the flood event (Table 3).

### 3.2. Geomorphological analysis

#### 3.2.1. Channel width, island and floodplain changes

Changes in channel width, islands and floodplains induced by the 2015 flood were assessed by field surveys and remote sensing analysis in both the nine tributaries and the Nure River. The remote sensing analysis, based on two sets of orthophotos taken before and after the flood (Fig. 2a and b) and topographic maps at the 1:5000 scale, was carried out using a GIS software (ESRI ArcGIS ver.10.4). Pre-flood orthophotos (ground resolution of 0.5 m) were taken in 2011 but are considered representative of the channel at the time of the event because geomorphically effective floods did not occur between 2011 and September 2015, as confirmed by available imagery on Google Earth© referring to October 2014. Post-flood orthophotos

Table 2

River	N	L (m) min–max	$W_{pre}$ (m) min–max	$W_{post}$ (m) min–max	WR average	$F_{pre}$ (m) min–max	$F_{post}$ (m) min–max	FR average
Nure	48	400–1370	2.5–12.9	45.2–70.7	1.7	31–342	21–303	−0.25
Lobbia	17	140–300	3–24.7	5.1–68.4	3.3	3–151	0–121	−0.65
Lamazze	11	140–320	1.5–2.4	6.3–12.4	4.7	5–30	0–8	−0.93
Piva	12	120–230	1.3–3.7	5–14	4.1	5–14	0–7	−0.75
Grondana	18	110–500			4.5	1–103	0–23	−0.72
Riccó	21	115–215	1.4–13	5.8–59	5.1	5–50	0–11	−0.75
Lavaiana	15	180–540	3.2–77.6	10–102.6	1.6	11–95	8–83	−0.19
Cavala	8	150–230	7.7–40	10.5–43.5	1.4	2–28	1–22	−0.35
Lardana	16	290–540	1.3–9.48	5.96–74.3	3.4	15–170	0–134	−0.54
Riazzo	9	185–320	2.4–9	5.5–38.2	2.7	3.5–132	0–101	−0.63

Codes: N, number of sub-reaches for each river; L, length of sub-reaches;  $W_{pre}$ , channel width before the flood;  $W_{post}$ , channel width after the flood; WR, width ratio;  $F_{pre}$ , floodplain width before the flood;  $F_{post}$ , floodplain width after the flood; FR, floodplain ratio.

Table 3

Variable	Symbol	Description
Average channel width before the flood (m)	$W_{pre}$	Ratio between channel sub-reach polygon area before the flood and its length. Islands are excluded from the computation
Average channel width after the flood (m)	$W_{post}$	Ratio between channel sub-reach polygon area after the flood and its length. Islands are excluded from the computation
Width ratio (m/m)	WR	Ratio between channel width after the flood and channel width before.
Channel slope (m/m)	Sc	Channel slope
Bed level modification (m)	CBL	Difference e in average bed elevation derived from multi-temporal cross-sections
Average floodplain width before the flood (m)	$F_{pre}$	Ratio between polygon floodplain area associated to the sub-reach before the flood and the sub-reach length.
Average floodplain width after the flood (m)	$F_{post}$	Ratio between polygon floodplain area associated to the sub-reach after the flood and the sub-reach length.
Floodplain ratio (m/m)	FR	Ratio between floodplain width after the flood and floodplain width before.
Floodplain elevation modification (m)	FL	Difference in average floodplain elevation derived from multi-temporal cross-sections
Valley width (m)	V	Width of valley bottom evaluated as the ratio between the valley polygon area and its length
Islands area before the flood (m <sup>2</sup> )	$I_{pre}$	Area of islands in the sub-reach before the flood
Island area after the flood (m <sup>2</sup> )	$I_{post}$	Area of islands in the sub-reach after the flood
Number of islands before the flood	$nI_{pre}$	Number of islands before the flood
Number of islands after the flood	$nI_{post}$	Number of islands after the flood
Confinement index (m/m)	CI	Ratio between alluvial plain width and the channel width before the flood (Rinaldi et al., 2013)
Basin area (km <sup>2</sup> )	Ba	Drainage area relative to each sub-reach.
Sediment Supply (m <sup>2</sup> )	SS	Landslide areas coupled to the main channel network
Average cumulative rainfall (mm)	R	Average cumulative rainfall in the catchment draining the sub-reach
Peak Discharge (m <sup>3</sup> s <sup>−1</sup> )	$Q_{pk}$	Peak discharge reconstructed by modelling and topographic survey
Total stream Power	$\Omega$	total stream power $\Omega = \gamma QS$ ; $\gamma$ is the specific weight of water (Nm <sup>−3</sup> ), $Q$ is the discharge (m <sup>3</sup> s <sup>−1</sup> ), and $S$ is channel slope (Bagnold, 1966; Magilligan, 1992, Knighton, 1999; Reinfelds et al., 2004)
Unit stream power pre flood (m <sup>3</sup> s <sup>−1</sup> km <sup>−2</sup> )	$\omega_{pre}$	$\omega = \Omega / W_{pre}$
Unit stream power post flood (m <sup>3</sup> s <sup>−1</sup> km <sup>−2</sup> )	$\omega_{post}$	$\omega = \Omega / W_{post}$

(ground resolution of 0.2 m) were taken on 25th October 2015 a few weeks after the flood.

Channel margins, islands and alluvial plain margins, were digitized from both pre- and post-flood orthophotos (Toone et al., 2012; Surian et al., 2016). Changes in channel width, induced by the 2015 flood, were expressed by the width ratio (WR) computed as the ratio between the channel width after and the channel width before the flood (Krapesch et al., 2011). Channel width evaluation, and consequently the width ratio, are affected by errors related to orthophoto interpretation and polygon digitalization, and overall the absolute error is estimated to be in the order of few meters. These errors are negligible if compared to the observed changes in channel width (Table 2). Additional morphological parameters were assessed to characterize the morphology of each sub-reach and to define their modification induced by the flood as defined in Table 3.

### 3.2.2. Channel bed elevation changes

Flood-related bed level variations were assessed by field surveys and through cross-sections surveyed before and after the flood. Two separate approaches were used for the Nure River and the tributaries. In the Nure River, bed elevation changes were derived by the comparison of 47 cross-sections (see Fig. 1a for location) surveyed in 2007 with cross-sections extracted from an ALS-derived Digital Terrain Model (DTM), with a resolution of 1 m, obtained after the flood (Fig. 2c). Average active bed elevations for each cross-section before and after the flood event were computed. The pre-event cross-sectional surveys were considered representative of the channel bed level before the event because no geomorphically-effective floods occurred between 2007 and September 2015 floods. A threshold of  $\pm 0.5$  m for defining significant changes of bed-level was assigned. Indeed, since LiDAR-derived cross-sections do not represent the actual bed elevation within the wetted portion of the active channel, post-flood aggradation in the Nure might be over-estimated. Nonetheless, it was verified that water depth during the ALS did not exceed 0.30 m. Therefore, the incision was defined when the elevation difference was  $< -0.5$  m and aggradation when  $> 0.5$  m. Conversely, “Stable” (i.e. limited bed elevation changes) conditions were considered in the range  $-0.5$  to  $+0.5$  m. In the tributaries, topographic cross-sections and detailed LiDAR post-event were not available, but vertical changes were estimated during the field surveys in 14 selected sub-reaches (Fig. 1a). These estimations used evidence of aggradation and incision such as buried trees (Fig. 2d), burial/exposure of buildings, presence of depositional lobes (Fig. 2e and f), elevation difference between the former floodplain and the newly formed bars.



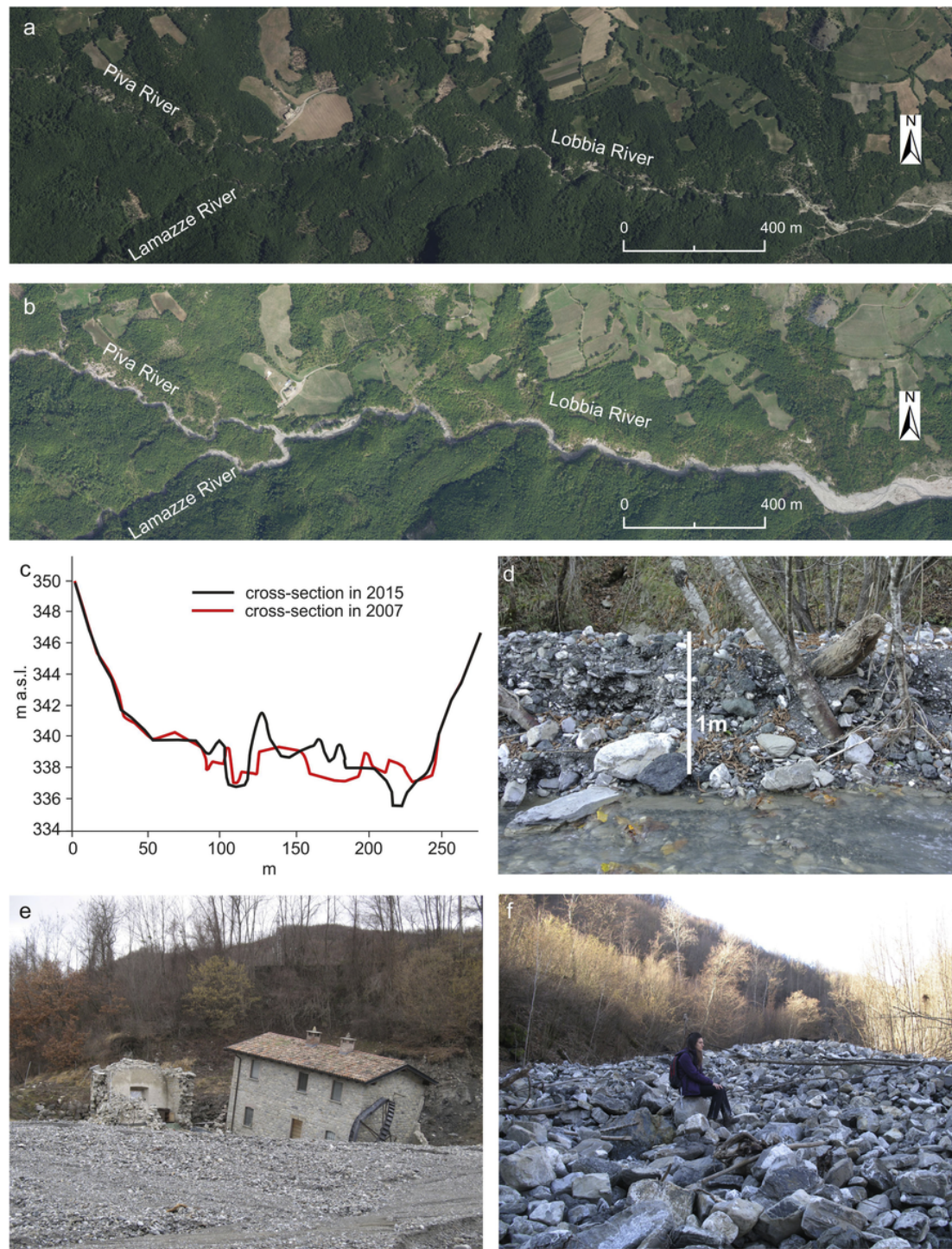


**Fig. 2.** Orthophoto of 2011 (a), and immediately the post-flood event (b) in the Lobbia, Piva and Lamazze rivers showing changes in channel width after the flood. Comparison of cross-sections surveyed before and after the flood event (c). Insights of floodplain aggradations in the Lamazze River (d); of floodplain and channel aggradation in the Grondana River (e); depositional lobe in the Lamazze River (f).

### 3.2.3. Sediment sources and connectivity

The landslide inventory related to the 15th September 2015 event was produced through field surveys and interpretation and comparison of orthophotos taken before (i.e. orthophotos 2011 at 0.5 m resolution and Google Earth© images 2014) and immediately after the

flood (i.e. orthophotos 25th September 2015 at 0.2 m resolution). Field surveys were also supported by the analysis of satellite images acquired between 18th and 21st September 2015 (<http://emergency.copernicus.eu/mapping/list-of-components/EMSR136>). Both the most likely initiation site and the boundaries of the deposits were mapped in GIS.

The assessment of sediment supplied from the hillslopes to the channel network during the flood was carried out following the procedure presented in Surian et al. (2016), which encompasses the geomorphometric analysis of the mapped sediment sources and the calculation of an index of sediment supply expressed by the total sediment source planar area connected to each sub-reach. In order to evaluate the areas responsible for sediment supply, a map of the sediment connectivity index (Cavalli et al., 2013) computed by means of the SedIn-Connect software (Crema and Cavalli, 2018) was overlaid on the landslides map.

### 3.3. Hydrological-hydraulic analysis

#### 3.3.1. Quantitative estimation of spatially-distributed rainfall and recorded flood hydrographs

Spatially distributed rainfall estimates for the September 2015 event were obtained from the C-Band weather radar located at Settepani (ARPA Piemonte), 100–120 km away from the catchment. Radar data were available at 10 min temporal resolution and were processed for the removal of non-precipitating echoes (Doppler-based filter), to correct the errors due to partial beam blockage (Pellarin et al., 2002) up to 70% power loss, as recommended by Marra et al. (2014), and to beam attenuation in heavy rain (Marra and Morin, 2015). Rainfall rate ( $R$ ) was calculated from radar reflectivity ( $Z$ ) using a power law relation in the form  $Z=300 R^{1.5}$ , well suited for convective-type rainfall. Data was produced in 500 m  $\times$  500 m Cartesian grids and a limited number of missing scans was interpolated from the closest available data. The final radar quantitative precipitation estimation was produced with two adjustment steps including a multi-quadratic spatial dependent adjustment and a mean filed bias adjustment based (Borga et al., 2000) on rain gauge measurements (Martens et al., 2013; Amponsah et al., 2016). Rain gauge data was provided at 30 min resolution for a total of 27 rain gauges (ARPAE Emilia Romagna, 2016). Assessment of the final estimates shows a good spatial representation of the storm-scale rainfall amounts (correlation coefficient up to 0.9), and of the total rainfall volumes (2% relative bias).

Three stream gauging stations on the Nure River were operational during the flood of 13–14 September 2015: Ferriere (48 km<sup>2</sup>), Farini (208 km<sup>2</sup>), Ponte dell'Olio (337 km<sup>2</sup>) (Fig. 1b). The records at Ferriere and Farini have gaps around the flood peak, which has been reconstructed after the event from the flood marks (ARPAE Emilia Romagna, 2016). No suitable flow rating curves were available for any gauging station to determine the September 2015 flood peak. The flood hydrograph at Farini was reconstructed by means of a hydrodynamic numerical model (Mignosa et al., 2015).

#### 3.3.2. Post-flood reconstruction of peak discharge

The assessment of flood response along the main stream and on the tributaries required the indirect reconstruction of peak discharge at several ungauged cross sections. The core of the implemented approach consists in the topographic survey of channel reaches hit by the flood, with special attention to the recognition of high water marks, and computation of the peak discharge by means of the Manning-Strickler equation under the assumption of uniform flow (Gaume and Borga, 2008). The uncertainties in indirect peak discharge assessment resulting from measurement errors, estimation of the roughness coefficient, and geomorphic changes of the cross sections were assessed according to the method proposed by Amponsah et al. (2016). The peak discharge was estimated at ten sites, two of them on the Nure and the remaining ones on tributaries draining areas

from 1.8 to 30 km<sup>2</sup>. The geomorphic effects of the flood (channel widening, incision, and within channel sedimentation) were surveyed and ranked into three classes according to the severity of caused changes: *Major*, *Small to Moderate*, and *Negligible* (Marchi et al., 2016).

The estimation of flow velocity and peak discharge in one steep channel, most likely affected by hyperconcentrated flow (Riccò Creek), was performed by applying the vortex equation to lateral superelevation in bends (Costa, 1984; Scheidl et al., 2015). Because of the complex morphology of the surveyed channel reach, and the problems intrinsic to the application of the vortex equation to the reconstruction of velocity of flows with high sediment concentration (Prochaska et al., 2008), the peak discharge computed for the Riccò should be considered as a rough, approximate estimation.

#### 3.3.3. Flood response modelling

A distributed hydrological model was applied to analyze the flood response and to compute the flood peak discharge for the different channel reaches. We applied the Kinematic Local Excess Model – KLEM (Borga et al., 2007; Amponsah et al., 2016) that combines runoff generation by means of the Soil Conservation Service Curve Number (Ponce and Hawkins, 1996) with a network-based hillslope and channel runoff propagation model.

The model was calibrated on the Nure River at Farini by comparing model-simulated discharge with the flood hydrograph reconstructed by Mignosa et al. (2015). The hydrological model was verified by comparing model-simulated flood peaks with peak discharges reconstructed after the flood at the ungauged cross sections. Model parameters were transposed to the basins related to the cross sections where peak discharge has been estimated from the flood marks. The KLEM model was then applied at the channel reach scale to compute peak discharge (and hence stream power).

Flood propagation on the main Nure channel was simulated by using the HEC-RAS code (Hydrologic Engineering Center 2001) for unsteady open channel flow (Saint Venant equations).

### 3.4. Controlling factors for channel width changes

The influence of a number of potential controlling factors on channel changes caused by the flood event was analyzed. The morphological variables and hydrological and hydraulic factors reported in Table 3 were considered. The whole database (175 sub-reaches) was split into two subsets on the basis of channel confinement after the flood, expressed by the equation:

$$W^* = W_{post}/V$$

where  $W_{post}$  is the channel width after the event and  $V$  is the valley width (see Table 3). Two datasets differing for the residual potential of erodible width beside the channel were created. Two datasets were identified based on post-flood channel confinement. In the first dataset (hereafter Dataset 1, 36 sub-reaches), characterized by small and more confined streams, the channel width after the flood was almost equal to the valley width ( $W^* \geq 0.9$ ), while, in the second dataset (hereafter Dataset 2, 139 sub-reaches), which includes larger and less confined streams, the widening was not large enough to occupy almost entirely the valley floor ( $W^* < 0.9$ ). Simple and multiple linear regression analyses between channel planform, vertical changes, and morphological/hydraulic variables were performed using the software R (version 3.2.3).

## 4. Results

### 4.1. Rainfall and flood response analysis

The cumulative rainfall depth (Fig. 3) ranged from 60 to 360 mm in 12 h over the analyzed area. Fig. 4a shows that basin averaged cumulative rainfall was 150–180 mm for the Cavala, Lavaiana, and Piva basins, while it exceeded 200 mm (and in some cases > 250 mm) in the Riazzo, Grondana, Lardana and Riccò basins, in the upper part of the Nure basin. Cumulative precipitation >180 mm corresponds to recurrence intervals exceeding 150 years for all durations relevant for the storm (from 3 h to 12 h), based on estimates obtained using the Ferriere rain gauge station (64 years of maximum annual rainfall data series). For the same durations and station (relatively close to the Cavala, Lavaiana and Piva basin), 150–180 mm are associated with recurrence intervals in the 100–150 years range.

Table 4 reports the peak discharge values reconstructed in ungauged cross sections after the flood and the related uncertainty bounds; the morphological changes in five out of ten cross sections were rated as *Major*, whereas four were classified as *Small to Moder-*

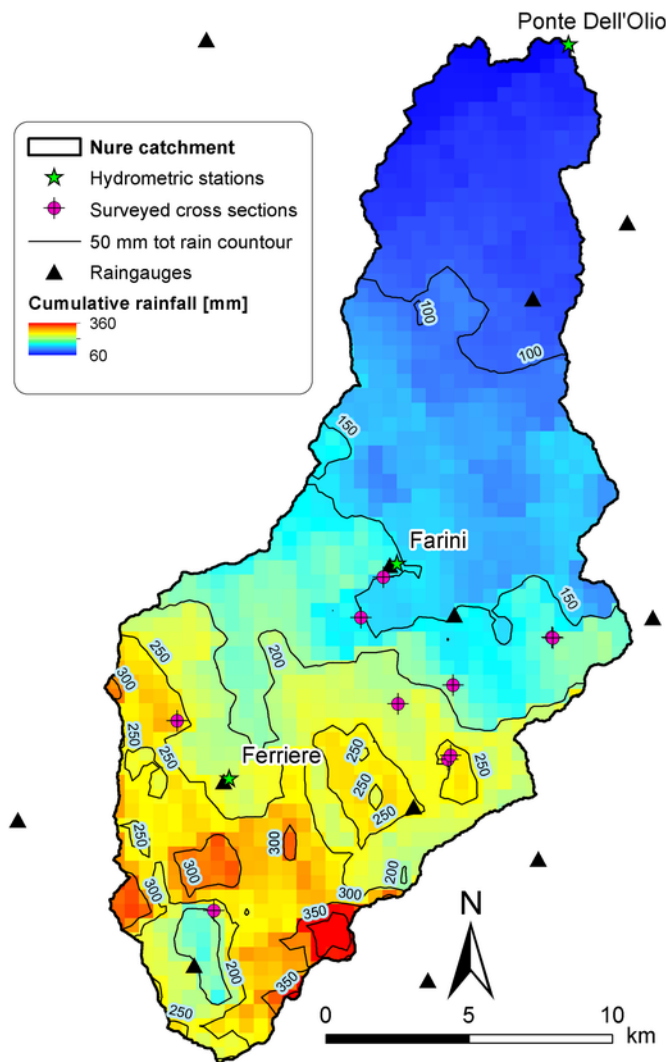


Fig. 3. Cumulative rainfall map of the 13–14 September 2015.

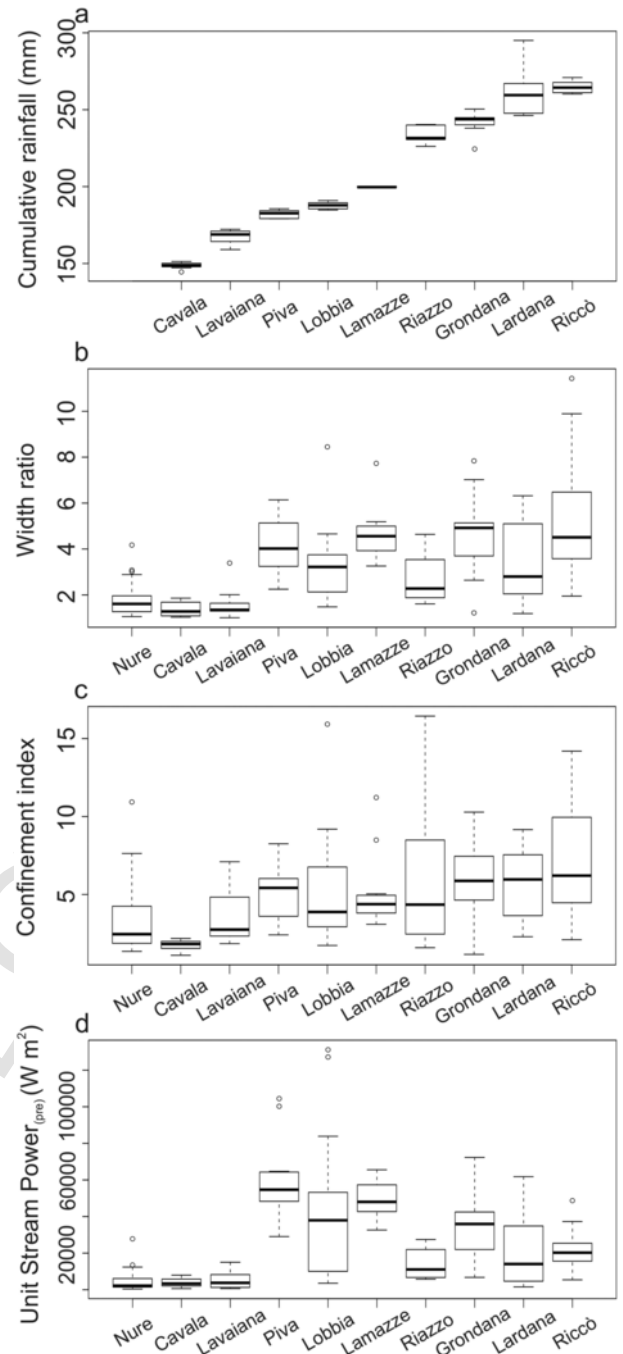


Fig. 4. Box and whiskers plots presenting median and interquartile range (25th and 75th percentiles), in the studied rivers of: average cumulative rainfall (a); width ratio (b); confinement index (c); unit stream power using pre-flood width (d).

ate, and only one as *Negligible*. Remarkably, the peak discharge estimated for the Nure at Farini shows a satisfactory agreement with the one independently obtained by Mignosa et al. (2015) by means of the application of hydrological and hydraulic models. In 6 out of 10 cross sections, the model simulated values of peak discharge falling within the uncertainty bound of field reconstructed values, thus with a performance similar to other extreme flash floods recently studied in Mediterranean basins (Amponsah et al., 2016).



**Table 4**

Flood response analysis: estimation of peak discharge in the upper Nure River basin.

River	Catchment area (km <sup>2</sup> )	Q peak (m <sup>3</sup> s <sup>-1</sup> )	Lower uncertainty bound	Upper uncertainty bound	Geomorphic effects	Code (Fig. 1b)
Nure at Rompeggio	22.8	135	104	166	Small-moderate	1
Grondana at Grondone di Sotto	8.7	175 <sup>a</sup>	110	240	Major	2
Lardana	29.8	155	97	213	Major	3
Lardana tributary	4.5	80	61	99	Small-moderate	4
upper Lardana	2.0	37 <sup>a</sup>	28	46	Small-moderate	5
upper Lardana	1.8	29 <sup>a</sup>	22	36	Small-moderate	6
Lavajana (left tributary)						
upper Lavajana (right tributary)	3.9	20 <sup>a</sup>	17	23	Negligible	7
Lavajana	26.6	180 <sup>a</sup>	113	247	Major	8
Lobbia	21.4	250	157	343	Major	9
Nure upstream of Farini	194.1	1760 <sup>a</sup>	1107	2413	Major	10

<sup>a</sup> Model-simulated discharge within the uncertainty bounds of post-flood field estimates.

## 4.2. Geomorphological changes induced by the flood

### 4.2.1. Morphological changes in channels, islands and floodplains

The most relevant morphological effect of the flood was channel widening (Fig. 4b and Table 2), with an average value of 18m and a maximum of 72m. Overall, widening was more intense in the channels which were narrower prior to the flood event (Fig. 5a) and in channels with higher average slope. Channel width ratio did not exceed 4 in the reaches with larger drainage areas (>20 km<sup>2</sup>; Fig. 5b).

Channel widening was often associated with channel pattern changes. In the tributaries, the prevalent sinuous and sinuous with alternate bars patterns before the flood were transformed into sinuous with alternate bars (from formerly sinuous), and wandering or braided morphologies after the flood. The Nure River, in the segments located upstream of the confluence with the Lardana River, was characterized by the shifting of its former sinuous pattern to sinuous with alternate bars and wandering types. In the downstream reaches, the Nure featured wandering and braided morphologies already prior to the 2015 flood, and no significant changes in planform morphology occurred.

Post-flood field surveys revealed that active channel widening was caused by three main processes: channel lateral migration through bank erosion; island erosion; overbank deposition of gravel and sand materials on the floodplain. In most cases, it was not possible to distinguish from the orthophotos if the widening was due to bank erosion or to overbank gravel deposition.

The widening was related to floodplain erosion in all the tributaries and to both floodplain erosion and island removal in the Nure and in some sub-reaches of the Lavaiana and Lardana rivers.

Floodplain erosion was observed in all sub-reaches (Table 2). On average, floodplain area decreased by about 52%. Floodplains were strongly eroded in the tributaries (Table 2), and in most reaches it was completely removed. Conversely, floodplain erosion was less intense in the Nure River (25% reduction on average, Table 2).

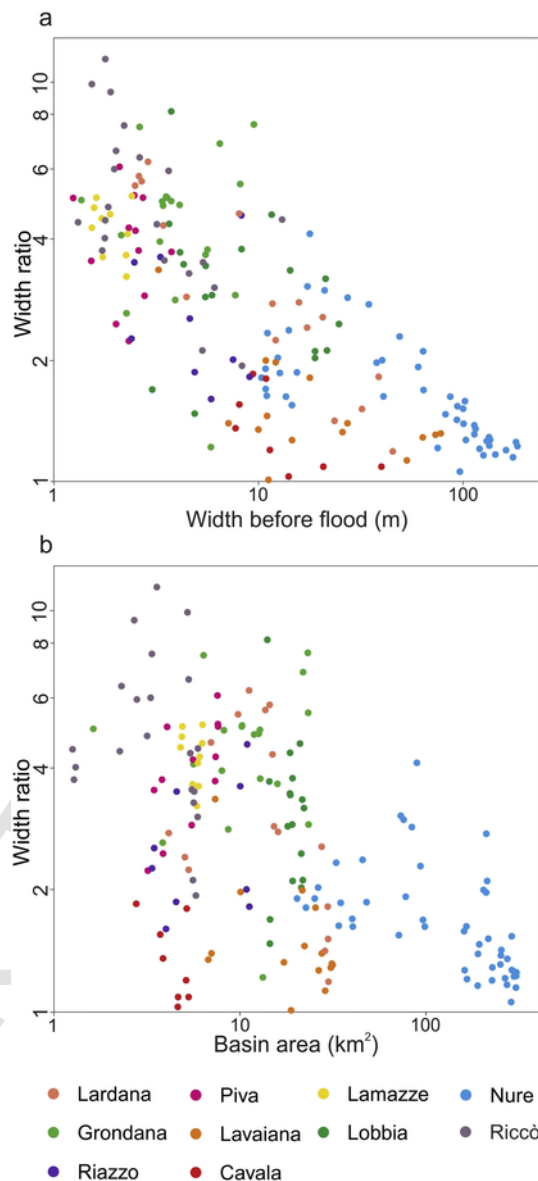


**Fig. 5.** Scatterplot of width ratio versus channel width before the flood event (a) and versus basin area (b).

Correlation analyses show that the floodplain erosion (measured by the floodplain ratio, i.e. ratio of floodplain area before and flood and after the flood) increases with higher unit stream power ( $r=0.58$ ,  $p\text{-value}<0.001$ , calculated using the pre-flood channel width), decreases in wider pre-flood channels ( $r=-0.54$   $p\text{-value}<0.001$ ) and for steeper channels ( $r=-0.63$   $p\text{-value}<0.001$ ).

Both an increase and a decrease of islands number were caused by flood (Fig. 6). In most of the tributaries, islands were completely removed. However, in some sub-reaches, new dissection islands (Gurnell et al., 2001) were formed as the result of the fragmentation of the former floodplain. A different behavior is evident in the Lavaiana River where islands remained quite stable, apart from a slight size reduction. Pre-existing islands were completely eroded in the Nure River, with a very limited number of newly formed islands.

Fig. 6 shows the relationship between width ratio and the processes of island erosion, formation and stability. Overall, widening was more intense in the sub-reaches also affected by the forma-

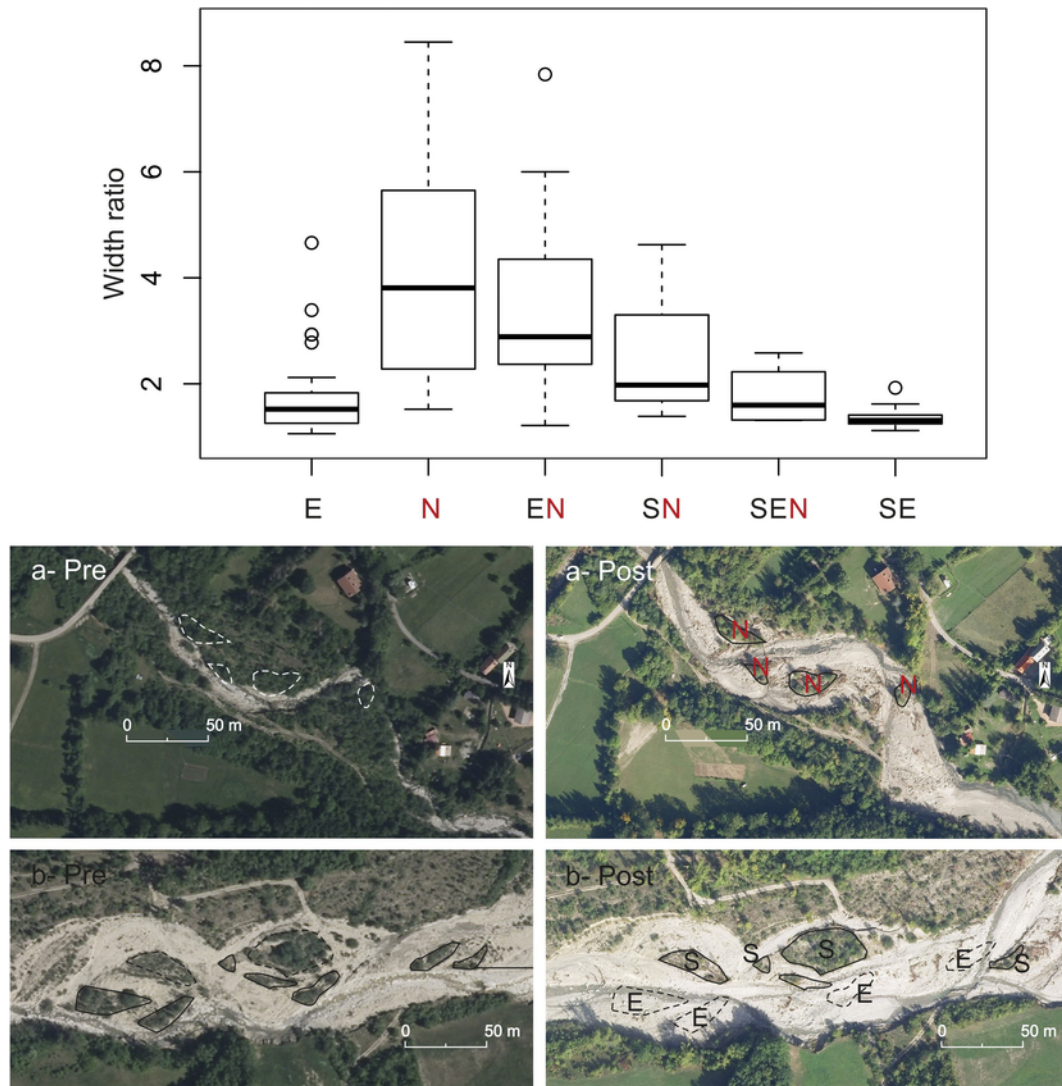


**Fig. 6.** Boxplots presenting median and interquartile range (25th and 75th) of width ratio for different processes affecting the island during the flood (erosion E; new formation N; stability S). In the x-axis, letters in black refer to island before the flood, in red to island formed after the flood. Codes: E=sub-reach characterized by pre-existent islands completely eroded after the flood; N=sub-reach characterized by new islands not present before the flood. EN=sub-reach characterized by islands completely new and not present before the flood, while all pre-existent islands were completely eroded after the flood; SN=sub-reach characterized by some new islands not present before the flood and by some stable islands already present before the flood. SEN=sub-reach characterized by some pre-existent islands completely eroded after the flood, some new islands not present before the flood and some islands already present before the flood. SE=sub-reach characterized by both, some pre-existent islands eroded after the flood and by some islands remaining quite stable after the flood. (For interpretation of the references to colour in this figure legend, the reader is referred to the web version of this article.)

tion of new islands after the flood event (N, EN and SN; Fig. 6). On the contrary, width ratio was minor in the reaches affected by prevalent island stability and erosion (E, SEN, SE; Fig. 6).

#### 4.2.2. Channel bed elevation changes

In the Nure River, 14 cross-sections underwent aggradation with average values ranging from +0.5 to +1.4 m; two cross-sections feature incision with values from -0.5 m to -0.8 m, and the remaining 31 cross-sections display stable conditions. Therefore, channel stability and aggradation were the dominant processes in the Nure River (Fig. 7a). Remarkably, the Nure reaches featuring the larger widening are approximately the same one experiencing the higher aggradation ( $r=0.46$ , Fig. 7b).

The best multiple regression model relating bed-level changes in the Nure River to hydraulic and morphological parameters includes the confinement index ( $CI$ ) and the unit stream power calculated us-

ing the *post-flood width* ( $\omega_{post}$ ), with the former being the most important variable (Table 5). The model indicates that aggradation was more intense in those sub-reaches characterized by the higher confinement index (i.e. wider valley floor), while confined sub-reaches underwent incision or remained stable (Fig. 7c). Incision took place in the sub-reaches having the higher values of unit stream power (Fig. 7d).

In the tributaries, channel aggradation was the prevalent vertical change (Fig. 7a). It was on average 1.0 m, and it ranged from 0.3 to 1.5 m (Fig. 7a), with the largest deposited clasts on average 0.45 m in diameter, but up to 2 m.

Field evidence allowed characterizing the deposits created by the flood event as composed by clast-supported pebbles, cobbles and boulders, poorly to moderately sorted, moderately to well imbricated and weakly stratified with alternating well to poorly sorted strata, in some cases presenting a matrix rich in coarse sand and granules. Bed-

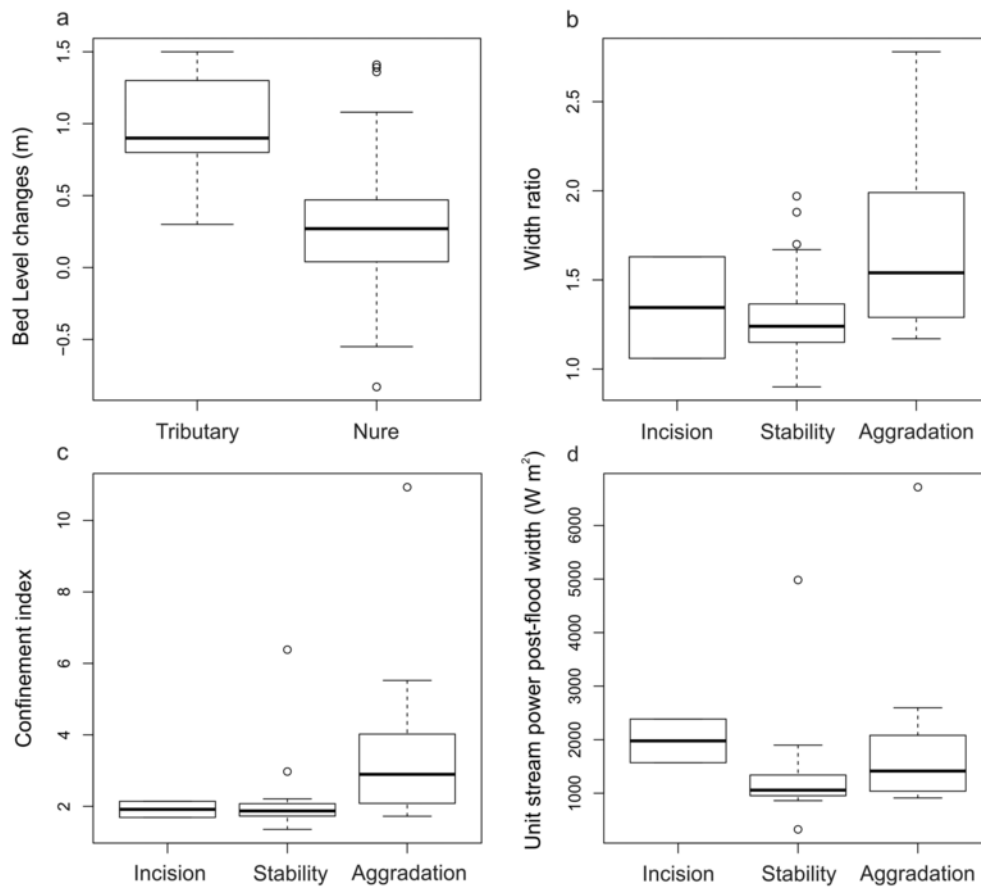


**Fig. 7.** Boxplot of bed level modification in the tributaries and in the Nure River (a); Boxplot of width ratio for bed-level type processes, in Nure River (b); Boxplot of confinement index for bed-level type processes, in the Nure River (c); Boxplot of unit stream power using post-flood width for bed-level type processes, in the Nure River (d). All plots present median and interquartile range (25th and 75th).

**Table 5**

	Model: Bed-level changes (Nure River)			Model: Wr (Dataset1)		Model: Wr (Dataset2)		
	Adjusted $R^2=0.46$ $p\text{-value}<0.001$			Adjusted $R^2=0.99$ $p\text{-value}<0.001$		Adjusted $R^2=0.63$ $p\text{-value}<0.001$		
	Intercept	CI	$\omega_{\text{post}}$	Intercept	CI	Intercept	CI	$\omega_{\text{pre}}$
Coefficient	0.07	0.44	-0.005	0.08	1.02	0.61	0.33	0.00003
$p\text{-value}$	—	<0.001	<0.001	—	<0.001	—	<0.001	<0.001
Relative importance metric	—	0.67	0.33	—	—	—	0.63	0.37

load – although very intense – was the most relevant transport process in all the tributaries apart from the Riccò Creek. Indeed, the presence of deposition lobes, of many large angular to sub-angular boulders sitting on finer layer, of alternating normal and poorer organized deposits, indicate that this creek was subjected to a non-Newtonian flow process, likely a hyperconcentrated flow (Costa, 1988).

#### 4.2.3. Sediment supply from hillslopes

In the upper Nure River basin, over an approximate area of 350 km<sup>2</sup>, the inventory of slope instability processes triggered during the September 2015 storm resulted in a total of 27 debris flows/debris floods and 9 debris slides.

According to the connectivity analysis (Section 3.2.3), all the sediment sources in the inventory are coupled to the channel network.

This means that all the landslides mapped in the inventory effectively contribute to sediment supply in the study reaches. According to the procedure presented in Surian et al. (2016), 33 out of the 127 analyzed reaches were affected by lateral sediment supply. Among them, 3 reaches of the Grondana Creek featured the highest value of sediment supply per unit channel length (194, 124, and 110 m<sup>2</sup> m<sup>-1</sup>), and several reaches of the Riccò Creek, along with 5 of the Grondana, 2 of the Lobbia and a reach in the Lamazze, exceed the value of 10 m<sup>2</sup> m<sup>-1</sup>. All reaches belonging to the Riazzo, Lavaiana and Lardana channels were not affected by sediment supply from the hillslopes.

#### 4.3. Controlling factors for channel width changes

Simple and multiple regression analyses were used to explore the relationship between widening and possible controlling factors in the two groups (Dataset 1 corresponds to small and more confined streams, whereas Dataset 2 corresponds to larger and less confined streams), whose main parameters are listed in Table 6. Due to non-Newtonian flow process characterizing Riccò Creek, sub-reaches belonging to the Riccò were excluded from the regression analysis.

The testing of simple and multiple regression models of the Dataset 1 indicated that channel widening was exclusively dependent on the confinement index (Table 5 and Fig. 8a), i.e. channels widened to occupy the entire the valley floor and hillslopes constrained further channel expansion.

Several multiple regression models were applied to the Dataset 2. The best model (Table 5) includes confinement index ( $CI$ ) and unit stream power based on pre-flood channel width ( $\omega_{pre}$ ). The different potential controlling factors explaining width ratio for Dataset 2 were also explored individually (Fig. 8). Rather surprisingly, confinement index explained the largest share of width ratio variance in this case, even if widening was not physically limited by the size of the alluvial plain. Some of statistical analysis are affected by spurious correlations (through the use of initial channel width in the width ratio), but the evaluation of its effects on the goodness-of-fit of the different models (see also Righini et al., 2017) is not addressed in this paper.

In the sub-catchment tributaries, the link between width ratio and the average cumulative precipitation at the sub-reach scale was also examined (Fig. 9a). An upper value of about 180 mm characterized the sub-reaches featuring width ratios  $<2$ , belonging to the Cavala and Lavaiana rivers (Fig. 9a). Indeed, the sub-reaches catchments that received  $<180$  mm (and thus featuring recurrence interval  $<150$  yr) presented statistically lower width ratio compared to those featuring  $>180$  mm (Mann–Whitney test,  $p$ -value  $<0.005$ ).

The relative proportion of alluvial plain occupied by the channel after the flood is an important, dimensionless morphological variable to consider, also for management purposes. Fig. 9b shows that channels in the sub-reaches belonging to the Dataset 1 (confined after the flood event) have occupied  $>90\%$  of the valley floor width, while those belonging to the unconfined dataset (still unconfined after the flood event) have expanded over the 20–80% of the alluvial plain width. The same rainfall threshold (180 mm) was considered in the two datasets to assess (through the Mann–Whitney test) whether differences in the proportion of the valley floor reworked by the flood might emerge. In the case of Dataset 1, sub-reaches with  $<180$  mm feature a median value of 92% rework of the valley floor, while for those  $>180$  mm the value rises to 99% and the difference is statistically significant ( $p$ -value = 0.04). For Dataset 2, the valley floor rework proportion is higher for sub-reaches that received  $>180$  mm (median values 66% vs 56%), but the significance level is slightly lower ( $p$ -value = 0.07).

Other insights concerning the geomorphic effectiveness of the flood are reported in Fig. 9c, which considers the percentage of the valley floor occupied by the channel after the flood event in relation to the valley width. In the narrower valleys ( $<20$  m), most of the channels after the event occupied most of the alluvial plain. In the wider valleys, the proportion of valley bottom reworked by the flood decreases with increasing valley widths (Fig. 9c).

## 5. Discussion

### 5.1. Flood morphological effects and controlling factors

In the Nure catchment, the geomorphic responses to the flood were variable in different sub-reaches and different modes of widening occurred. In most tributaries, widening was strictly related to floodplain bank erosion and deposition of bedload material on the floodplains. In the Nure sub-reaches, floodplain erosion took place but it was not the dominant processes as widening mostly occurred due to island erosion, which was also found by Buraas et al. (2014).

The observed width ratios are similar in magnitude to those found for other large floods (recurrence intervals  $>100$  years, often  $>200$  years) studied during the last years in Italy (Nardi and Rinaldi, 2015; Surian et al., 2016; Righini et al., 2017). The range of widening in the Nure's tributaries (drainage area  $<30$  km<sup>2</sup>, average channel width before the flood about 10 m) is comparable with that reported for the tributaries (drainage area  $<40$  km<sup>2</sup>, average channel width before the flood around 12 m) analyzed by Surian et al. (2016) and Righini et al. (2017). Also the lower width ratios found for the Nure River (drainage area about 300 km<sup>2</sup>, average width before the flood about 73 m) are very similar to those found in the Magra River (drainage area about 1000 km<sup>2</sup>, average width before the flood around 110 m, Nardi and Rinaldi, 2015).

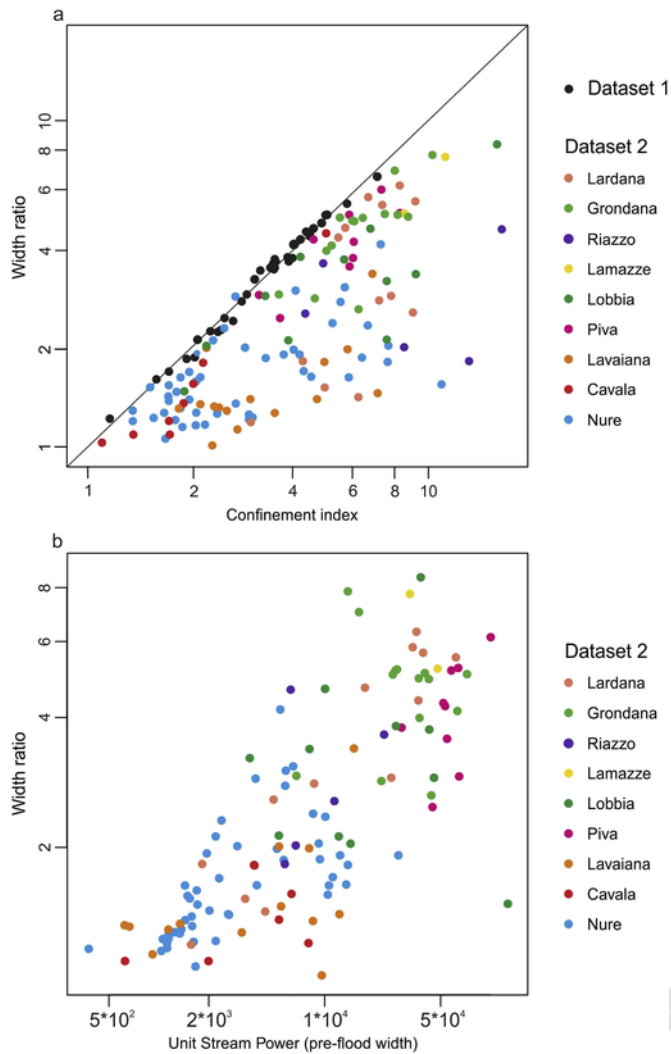
At the flood peak, unit stream power exceeded 380 W m<sup>-2</sup> in all studied channels, thus being beyond the 300 W m<sup>-2</sup> threshold proposed by Magilligan (1992) for relevant morphological changes, and far exceeding the 34 W m<sup>-2</sup> found by Bizzi and Lerner (2015) for bank erosion. However, as already found in previous studies, flood power alone can only explain part (up to about 50%) of the variability of observed channel widening (Heritage et al., 2004; Surian et al., 2016), confirming the extremely complex relationship between flood hydraulics and fluvial system response (Wohl et al., 1994; Heritage et al., 2004; Surian et al., 2016). Indeed, the addition of the confinement index to the unit stream power (calculated using the pre-flood width) increases importantly the regression model performance, and this index seems to bear the largest relevance for width changes also when widening is not enough to be physically constrained by the hillslopes. In other words, the lateral geomorphic effectiveness of the flood is strictly dependent on the availability of space (alluvial plain width). The same dominant controlling factors were identified by Surian et al. (2016) and Righini et al. (2017). While it is obvious that widening is limited by the valley plain width (as long as slopes are not eroded, see Surian et al., 2016 and Righini et al., 2017) in the narrower val-

Table 6

		$W_{pre}$	$W_{post}$	$Wr$	$Sc$	$FR$	$V$	$I_{pre}$	$I_{post}$	$CI$	$Ba$	$SS$	$Q_{pk}$	$\Omega$	$\omega_{pre}$	$\omega_{post}$
Dataset1	av	5.7	15.8	3.3	10.8	-0.94	16	35.1	118	3.3	9	1010	160	149,308	42,146	13,567
	min	1.5	5	1	3	-0.34	5	0	0	1.1	2.7	0	19	27,835	2146	1598
	max	25	61	5.6	21	-1	62	830	2	5.7	23	11,489	396	406,398	131,120	77,040
Dataset2	av	36.5	58	2.7	4.7	-0.4	109	3251	625	4.7	72	3639	558	127,380	16,802	5434
	min	1.5	5	1	0.01	-0.01	8	0	0	1.3	2	0	37	24,906	380	325
	max	184	228	8.5	21	-0.95	520	35,168	7197	16	306	136,191	1901	619,238	127,154	85,768

The Riccò Creek is excluded from the analysis.





**Fig. 8.** Scatterplot of width ratio versus confinement index for confined and unconfined reaches after the flood event (a); scatterplot of width ratio versus unit stream power using pre-flood width for Dataset 2 (b).

leys characterized by highly confined channels (Dataset 1), the reason behind the strong control exerted by the confinement index on width ratio on the channels not reaching the valley slopes (Dataset 2) during the flood is less clear.

Indeed, this study highlights a higher morphological sensitivity of the upstream, lower order reaches, characterized by narrower channels before the flood and steeper slopes (Fig. 5). These channels were, in some cases, partly confined before the flood (higher values of the confinement index, Fig. 4C). Remarkably, these channels occupied the entire valley bottom until the 1950s (based on historical maps and aerial photos), and underwent a subsequent narrowing trend possibly due to natural afforestation and climatic variations (Liébault and Piégay, 2002; Rinaldi et al., 2009; Bollati et al., 2014; Scorpio and Rosskopf, 2016; Marchese et al., 2017).

We believe that valley width – at least in unglaciated environments – is an indicator of how much a given river can expand during large, infrequent events or during sediment supply-rich periods. On the other hand, pre-flood channel width tends to correspond to bankfull conditions and thus to “ordinary” flood work. Therefore, relative channel widening is strictly related to the confinement index as the

latter integrates the river “expansion capacity” during extreme events relative to ordinary times.

Similar to what was found by Surian et al. (2016), sediment supply from hillslopes did not seem to play a relevant role in channel widening, although all landslides (mostly debris flows) connected with the river network. A possible reason may stem from the fact that the dominant coarse sediment input during the flood came from floodplain and island erosion, as landslides/debris flow volumes observed in the field were generally relatively small.

An important finding provided by this study, compared to the previous flood events analyzed in Italy, consists in the analysis of the bed-level vertical changes. In the Nure River incision took place where the valley bottom was very narrow. As expected, aggradation was associated to channel widening. Remarkably, bed-level changes in the Nure main channel are better described by the unit stream power calculated using the post-flood width ( $\omega_{post}$ ), whereas channel widening in the same river – as well as in all the earlier studies – features higher correlation with the unit stream power calculated using the pre-flood width. This might suggest that the widening process in the Nure River occurred earlier during the flood than bed level changes. Indeed, it is probable that in-channel sediment deposition took place during the receding limb of the hydrograph, due to a wider channel and to the (slower than water) arrival of intense bedload from the upstream reaches.

Furthermore, this study supports the current understanding that large floods control island type, spatial density and size, as put forward by Belletti et al. (2013). In most tributaries, new islands appeared after the flood as the result of the fragmentation of the floodplains. In the Nure River, islands were completely removed. Different from other rivers, in the Lavaiana, islands remained approximately stable although they were reshaped and slightly reduced in size. In the sub-reaches where unit stream power was higher (Fig. 10b), new islands appeared thanks to the formation of new lateral channels within the floodplain. In contrast, where unit stream powers were  $<10,000 \text{ W m}^{-2}$ , partial or complete island erosion was the dominant process, and new dissection islands could not form.

## 5.2. Basin-scale geomorphic changes distribution

In Fig. 10, the morphological changes variability at the catchment scale is illustrated along with the spatial distribution of rainfall, confinement index and unit stream power ( $\omega_{pre}$ ).

Extensive channel widening occurred especially in the middle-higher sectors of the Nure catchment. Both the Nure headwaters and its lower reaches were not quantitatively analyzed using remote sensing data, but during the field surveys; qualitative geomorphological analyses verified that important morphological changes did not occur there, despite very high precipitation and peak discharges. In headwater reaches, channel changes were probably limited by very confined, bedrock-dominated nature of the channel network. In downstream reaches, the negligible planform changes were likely due to the combination of low gradients (reducing unit stream power), cohesive bank material, and short flood duration.

In the analyzed channel network, both widening and aggradation were more pronounced in the tributaries (width ratio  $>2$ ; vertical changes  $>1 \text{ m}$ ) and especially downstream of the confluences (see the confluences between the Piva and Lamazze and between Grondana and Riccò in Fig. 10a). Similar geomorphological effects were described also in other studies (Petts and Gurnell, 2005; Ferguson and Hoey, 2008; Dean and Schmidt, 2013).

In the Nure River, widening was generally less marked, also downstream of confluences (Fig. 10a and c; Lardana, Lavaiana, Lob-

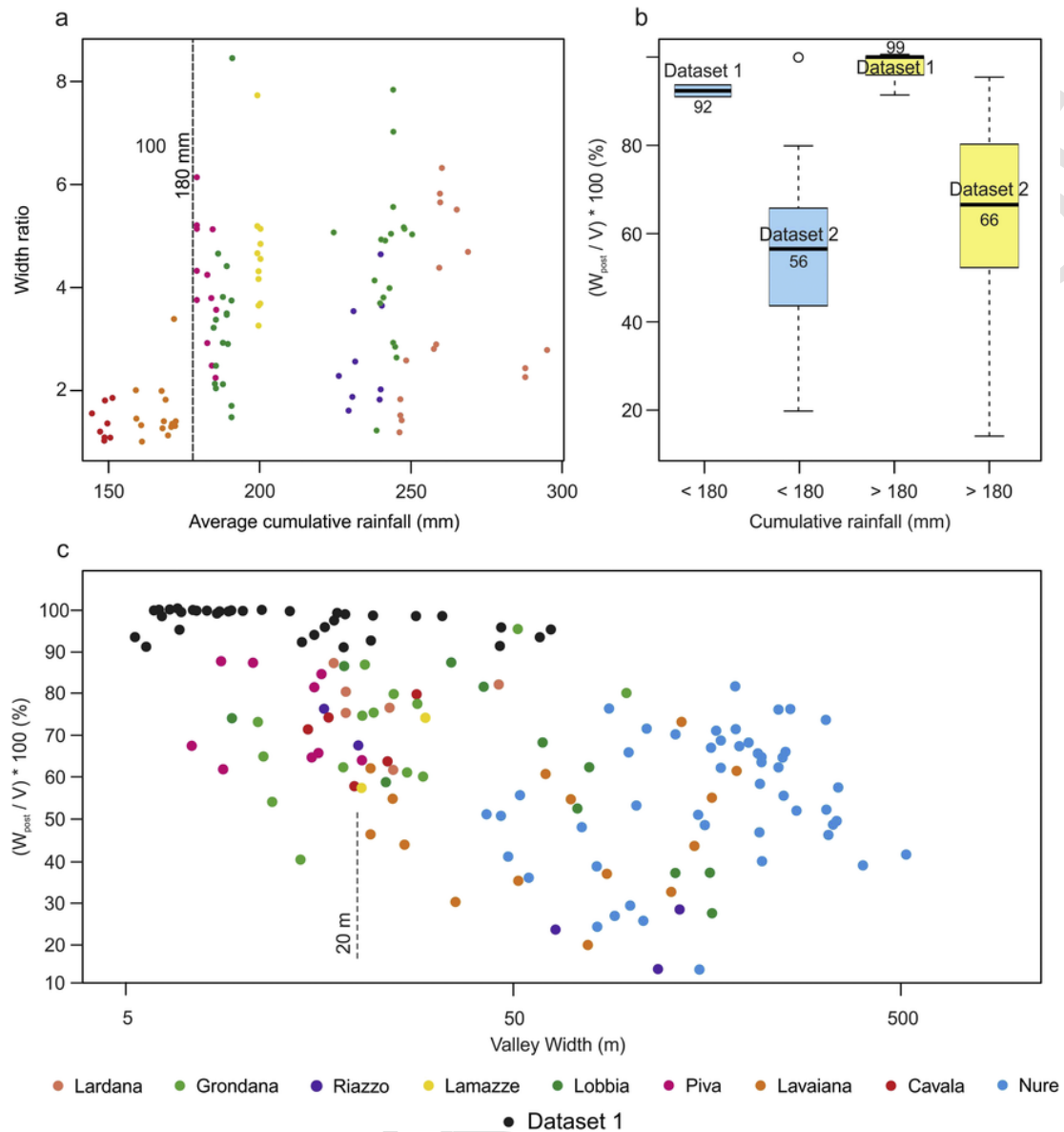


**Fig. 9.** Scatterplot of width ratio versus average cumulative rainfall, in the studied sub-reaches (a); Boxplot of ratio between the channel width after the flood event and valley width, for different ranges of cumulative precipitations, in Dataset 1 and Dataset 2. Plots present median and interquartile range (25th and 75th) (b); Simple regression between the ratio between the channel width after the flood event and valley width and the average valley width (c).

bia). On the contrary, bed instability and especially some aggradation and bar formation were found downstream of the junctions with the Lardana, Lavaiana, Lobbia (upward arrows in Fig. 10a and c).

At the basin scale, the relationship between the distribution of morphological changes and of controlling factors (Figs. 4 and 10b) shows strong overlap. The tributary reaches where the vertical changes were most dramatic correspond to those featuring the higher stream powers and greater lateral mobility (Figs. 4 and 10). A sharp reduction in geomorphic response is noted when passing from the tributaries to the main Nure channel. In the Nure River upstream of the confluence with the Lavaiana, widening is tightly related to the confinement index and to the increase in unit stream power immediately downstream of the tributaries (Fig. 10); moving downstream, channel changes become minor (Figs. 4 and 10).

As information on recurrence intervals related to peak discharges are not available for the tributaries, it is valuable to consider the pre-

cipitation amounts to infer the statistical relevance of such flood event in the different streams. In fact, on the contrary of other channels receiving higher amount of average cumulative rainfall (>180–200 mm), the Lavaiana and Cavala river basins feature the lowest rainfall amounts (<180 mm; recurrence interval <100–150 yr; Figs. 4, 9a and 10) and present also less marked morphological effects in terms of width ratio and island erosion.

### 5.3. Implication for flood hazard management

Flood hazard is not only related to water inundation but also to the geomorphic impacts of bank erosion and sediment deposition, which, if some anthropic structures are present, can cause damage or destruction (Hooke, 2015; Guan et al., 2016). This notwithstanding, neither hydraulic flood risk modelling and mapping nor the EU 'Floods

s (a); spatial distributions of  
s of width ratio, bed level n

This study provides some insights into the perspective of river management in valley settings similar to the Nure River basin, and improves our knowledge concerning the minimum demand of river space. Several methods were proposed for defining and mapping zones of possible channel mobility in the perspectives of river management (e.g. the ‘Erodible Corridor Concept’ by Piégay et al., 2005; the ‘Freedom Space for Rivers’ by Biron et al., 2014 and the ‘Event morphodynamic corridor’ by Rinaldi et al., 2015).

For instance, it emerged that widening decreases with increases in valley width (Fig. 9c). In narrower channels, processes of erosion and flooding take place in the floodplains and in the islands. Along such streams, flood hazard is very high in the whole valley bottom, in relation to both water inundation and sediment erosion and deposition. In wider valley bottoms, floodplains are more susceptible to water inundation. Erosion takes place especially within the channel (i.e. island removal) and only on relatively small portions of the floodplain. Nevertheless, it is worth noting that bank erosion can be of the order of tens of meters (e.g. it was up to 50m in some reaches on the Nure River), causing notable damages to building and infrastructure in wider valley bottoms.

## 6. Conclusions

This study confirmed that an integrated geomorphological and hydrological-hydraulic approach is fundamental for collecting and analyzing data on flood events in mountain channels. The main results can be summarized as follows:

- Geomorphic effects in the tributaries were characterized by intense to extreme changes in channel width associated with channel aggradation up to 2 m, removal of riparian vegetation, and changes in channel pattern. New islands were produced by fragmentation of the former floodplain.
- The morphological impact of the flood along the main river was less intense. It consisted in channel widening, mostly due to island erosion. Effects of bed level changes were varied, including aggradation, incision, and stability.
- Valley confinement represented the key controlling factor for channel widening with maximum unit stream power playing a role only in the unconfined channels.
- At catchment scale, the geomorphic effectiveness of the flood was more relevant in the middle-higher portions of the basin, where a higher amount of average cumulative rainfall was recorded.
- The study provided insights into the perspective of river management especially in relation to the definition of minimum spatial demand by the channel during an extreme flood and of the erosion processes involving the islands and the floodplains.

## Uncited references

Lane et al., 2007  
Neuhold et al., 2009  
Slater et al., 2015

## Acknowledgments

Funding for the lead author's work comes from the research projects ETSCH-2000 and FHARMOR (Autonomous Province of Bozen-Bolzano). The authors are grateful to the Agenzia interregionale per il Fiume Po and to the Regione Emilia-Romagna for providing maps, orthophotos, LiDAR data and cross-sections.

Authors thank Andrea Brenna, Ana Lucia Vela and Prof. Luisa Pellegrini for their support during the field surveys, Fabio Cancel and Giorgia Messina for supporting remote sensing data editing and Jay Frenress for the revision of the English language.

## References

- Amponsah, W., Marchi, L., Zoccatelli, D., Boni, G., Cavalli, M., Comiti, F., Crema, S., Lucia, A., Marra, F., Borga, M., 2016. Hydrometeorological characterisation of a flash flood associated with major geomorphic effects: Assessment of peak discharge uncertainties and analysis of the runoff response. *J. Hydrometeorol.* 17, 3063–3077. <https://doi.org/10.1175/JHM-D-16-0081.1>.
- Arnaud-Fassetta, G., Cossart, E., Fort, M., 2005. Hydro-geomorphic hazards and impact of man-made structures during the catastrophic flood of June 2000 in the Upper Guil catchment (Queyras, Southern French Alps). *Geomorphology* 66, 41–67.
- ARPAE Emilia Romagna, 2016. Servizio Idro Meteo Clima, Servizio Sismico, Geologico e dei Suoli. Rapporto sull'evento alluvionale del 14 settembre 2015. Unpublished report, (44 p., in Italian).
- Belletti, B., Dufour, S., Piégay, H., 2013. What is the relative effect of space and time to explain the braided river width and island patterns at a regional scale?. *River Res. Appl.* <https://doi.org/10.1002/rra.2714>.
- Belletti, B., Dufour, S., Piégay, H., 2014. Regional assessment of the multi-decadal changes in braided riverscapes following large floods (example of 12 reaches in South East of France). *Adv. Geosci.* 37, 57–71. <https://doi.org/10.5194/adgeo-37-57-2014>.
- Biron, P.M., Buffin-Bélanger, T., Larocque, M., Choné, G., Cloutier, C.-A., Ouellet, M.-A., Demers, S., Olsen, T., Desjarlais, C., Eyquem, J., 2014. Freedom space for rivers: a sustainable management approach to enhance river resilience. *Environ. Manag.* 54 (5), 1056–1073.
- Bizzi, S., Lerner, D.N., 2015. The use of stream power as an indicator of channel sensitivity to erosion and deposition processes. *River Res. Appl.* 31, 16–27. <https://doi.org/10.1002/rra.2717>.
- Bollati, I.M., Pellegrini, L., Rinaldi, M., Duci, G., Pelfini, M., 2014. Reach-scale morphological adjustments and stages of channel evolution: the case of the Trebbia River (northern Italy). *Geomorphology* 221, 176–186.
- Borga, M., Anagnostou, M., Frank, E., 2000. On the use of radar rainfall estimates for flood prediction in mountainous basins. *J. Geophys. Res.* 105 (D2), 2269–2280.
- Borga, M., Boscolo, P., Zanoni, F., Sangati, M., 2007. Hydrometeorological analysis of the 29 August 2003 flash flood in the eastern Italian Alps. *J. Hydrometeorol.* 8, 1049–1067. <https://doi.org/10.1175/JHM593.1>.
- Brierley, G.J., Fryirs, K.A., 2005. *Geomorphology and River Management: Applications of the River Style Framework*. Blackwell, Oxford.
- Buraas, E.M., Renshaw, C.E., Magilligan, F.J., Dade, W.B., 2014. Impact of reach geometry on stream channel sensitivity to extreme floods. *Earth Surf. Process. Landf.* 39, 1778–1789.
- Cavalli, M., Trevisani, S., Comiti, F., Marchi, L., 2013. Geomorphometric assessment of spatial sediment connectivity in small Alpine catchments. In: *Geomorphology, Sediment Sources, Source-to-sink Fluxes and Sedimentary Budgets*. vol. 188, pp. 31–41. <https://doi.org/10.1016/j.geomorph.2012.05.007>.
- Cenderelli, D., Wohl, E., 2003. Flow hydraulics and geomorphic effects of glacial-lake outburst floods in the Mount Everest Region, Nepal. *Earth Surf. Process. Landf.* 28, 385–407.
- Comiti, F., Da Canal, M., Surian, N., Mao, L., Picco, L., Lenzi, M.A., 2011. Channel adjustments and vegetation cover dynamics in a large gravel bed river over the last 200 years. *Geomorphology* 125, 147–159.
- Comiti, F., Lucia, A., Rickenmann, D., 2016. Large wood recruitment and transport during large floods: a review. *Geomorphology* 269, 23–39.
- Costa, J.E., 1984. Physical geomorphology of debris flows. In: Costa, J.E., Fleisher, P.J. (Eds.), *Developments and applications of Geomorphology*. Springer-Verlag, Berlin - Heidelberg, pp. 268–317.
- Costa, J.E., 1988. Rheologic, geomorphic, and sedimentologic differentiation of water floods, hyperconcentrated flows, and debris flows. In: Baker, V.R., Kochel, R.C., Patton, P.C. (Eds.), *Flood Geomorphology*. New York: Wiley, pp. 113–122.
- Costa, J.E., O'Connor, J.E., 1995. Geomorphically effective floods. In: Costa, J.E., Miller, A.J., Potter, K.W., Wilcock, P. (Eds.), *Natural and Anthropogenic Influences in Fluvial Geomorphology*. Monograph. vol. 89, American Geophysical Union, Washington, D.C., pp. 45–56.
- Crema, S., Cavalli, M., 2018. SedInConnect: a stand-alone, free and open source tool for the assessment of sediment connectivity. *Comput. Geosci.* 111, 39–45. <https://doi.org/10.1016/j.cageo.2017.10.009>.
- Dean, D.J., Schmidt, J.C., 2013. The geomorphic effectiveness of a large flood on the Rio Grande in the Big Bend region: insights on geomorphic controls and post-flood geomorphic response. *Geomorphology* 201, 183–198.
- European Commission, 2007. Directive 2007/60/EC of the European Parliament and of the Council of 23 October 2007 on the Assessment and Management of Flood Risks. *Off. J. (L 288/27)*, 6/11/2007, Brussels, Belgium, 8 pp.).
- Ferencevic, M.V., Ashmore, P., 2012. Creating and evaluating digital elevation model-based stream-power map as a stream assessment tool. *River Res. Appl.* 28, 1394–1416.
- Ferguson, R., Hoey, T., 2008. Effects of tributaries on main-channel geomorphology. In: Rice, S.P., Roy, A.G., Rhoads, B.L. (Eds.), *River Confluences, Tributaries and the Fluvial Network*. Wiley, London, pp. 183–208.
- Gaume, E., Borga, M., 2008. Post-flood field investigations in upland catchments after major flash floods: proposal of a methodology and illustrations. *J. Flood Risk Manage.* 1, 175–189. <https://doi.org/10.1111/j.1753-318X.2008.00023.x>.
- Grove, J.R., Croke, J., Thompson, C., 2013. Quantifying different riverbank erosion processes during 852 an extreme flood event. *Earth Surf. Process. Landf.* 38, 1393–1406. (Doi: 853 101002/esp3386).
- Guan, M., Carrivick, J.L., Wright, N.G., Sleight, P.A., Staines, K., E., H., 2016. Quantifying the combined effects of multiple extreme floods on river channel geometry and on flood hazards. *J. Hydrol.* 538, 256–268.
- Gurnell, A.M., Petts, G.E., Hannah, D.M., Smith, B.P.G., Edwards, P.J., Kollmann, J., Ward, J.V., Tockner, K., 2001. Riparian vegetation and island formation along the gravel-bed Fiume Tagliamento, Italy. *Earth Surf. Process. Landf.* 26, 31–62.
- Harvey, A.M., 2001. Coupling between hillslopes and channels in upland fluvial systems: implications for landscape. *Catena* 42, 225–250.
- Hauer, C., Habersack, H., 2009. Morphodynamics of a 1000-year flood in the Kamp River, Austria, and impacts on floodplain morphology. *Earth Surf. Process. Landf.* 34, 654–682. <https://doi.org/10.1002/esp.1763>.
- Heritage, G.L., Large, A.R.G., Moon, B.P., Jewitt, G., 2004. Channel hydraulics and geomorphic effects of an extreme flood event on the Sabie River, South Africa. *Catena* 58, 151–181.



- Hooke, J.M., 2015. Variations in flood magnitude–effect relations and the implications for flood risk assessment and river management. *Geomorphology* 263, 19–38.
- Hooke, J.M., 2016. Morphological impacts of flow events of varying magnitude on ephemeral channels in a semi-arid region. *Geomorphology* 252, 128–143.
- Hooke, J.M., Mant, J.M., 2000. Geomorphological impacts of a flood event on ephemeral channels in SE Spain. *Geomorphology* 34 (3–4), 163–180.
- Kale, V.S., 2007. Geomorphic effectiveness of extraordinary floods on three large rivers of the Indian Peninsula. *Geomorphology* 85, 306–316.
- Krapesch, G., Hauer, C., Habersack, H., 2011. Scale orientated analysis of river width changes due to extreme flood hazard. *Nat. Hazards Earth Syst. Sci.* 11, 2137–2147.
- Lallias-Tacon, S., Liébault, F., Piégay, H., 2017. Use of airborne LiDAR and historical aerial photos for characterising the history of braided river floodplain morphology and vegetation responses. *Catena* 149 (Part 3), 742–759.
- S.N.S.C., R.J.,
- Liébault, F., Piégay, H., 2002. Causes of 20th century channel narrowing in mountain and piedmont rivers of Southeastern France. *Earth Surf. Process. Landf.* 27, 425–444.
- Lucia, A., Comiti, F., Borga, M., Cavalli, M., Marchi, L., 2015. Dynamics of large wood during a flash flood in two mountain catchments. *Nat. Hazards Earth Syst. Sci.* 15, 1741–1755.
- Magilligan, F.J., 1992. Thresholds and the spatial variability of flood power during extreme floods. *Geomorphology* 5, 373–390.
- Magilligan, F.J., Phillips, J.D., James, L.A., Gomez, B., 1998. Geomorphic and sedimentological controls on the effectiveness of an extreme flood. *J. Geol.* 106 (1), 87–96.
- Magilligan, F.J., Buraas, E.M., Renshaw, C.E., 2015. The efficacy of stream power and flow duration on geomorphic responses to catastrophic flooding. *Geomorphology* 228, 175–188.
- Marchese, E., Scorpio, V., Fuller, I., McColl, S., Comiti, F., 2017. Morphological changes in Alpine rivers following the end of the Little Ice Age. *Geomorphology* 295, 811–826. <https://doi.org/10.1016/j.geomorph.2017.07.018>.
- Marchi, L., Cavalli, M., Amponsah, W., Borga, M., Crema, S., 2016. Upper limits of flash flood stream power in Europe. *Geomorphology* 272, 68–77.
- Marra, F., Morin, E., 2015. Use of radar QPE for the derivation of Intensity–Duration–Frequency curves in a range of climatic regimes. *J. Hydrol.* 531, 427–440. <https://doi.org/10.1016/j.jhydrol.2015.08.064>.
- Marra, F., Nikolopoulos, E.I., Creutin, J.D., Borga, M., 2014. Radar rainfall estimation for the identification of debris-flow occurrence thresholds. *J. Hydrol.* 519, 1607–1619. <https://doi.org/10.1016/j.jhydrol.2014.09.039>.
- Martens, B., Cabus, P., De Jongh, I., Verhoest, N.E.C., 2013. Merging weather radar observations with ground-based measurements of rainfall using an adaptive multi-quadratic surface fitting algorithm. *J. Hydrol.* 500, 84–96.
- Mignosa, P., Aureli, F., Ferrari, A., Prost, F., Vacondio, R., Capuano, F., Truffelli, G., Francia, C., 2015. Approfondimenti idrologici – idraulici a seguito dell'evento alluvionale del 13–14 settembre 2015 nel territorio del Comune di Farini, a supporto delle modifiche all'attuale assetto difensivo. Dipartimento di Ingegneria Civile, dell'Ambiente, del Territorio e Architettura – DICATeA, Università degli Studi di Parma and Servizio Tecnico dei Bacini degli affluenti del Po della regione Emilia – Romagna. Unpublished report, 103 p. (in Italian).
- Nardi, L., Rinaldi, M., 2015. Spatio-temporal patterns of channel changes in response to a major flood event: the case of the Magra River (central-northern Italy). *Earth Surf. Process. Landf.* 40, 326–339.
- Pellarin, T., Delrieu, G., Saulner, G.M., 2002. Hydrologic visibility of weather radar systems operating in mountainous regions: case study for the Ardèche catchment (France). *J. Hydrometeorol.* 3, 539–555.
- Petts, G.E., Gurnell, A.M., 2005. Dams and geomorphology: research progress and future directions. *Geomorphology* 71 (1–2), 27–47.
- Piégay, H., Darby, S.E., Mosselman, E., Surian, N., 2005. A review of techniques available for delimiting the erodible river corridor: a sustainable approach to managing bank erosion. *River Res. Appl.* 21 (7), 773–789.
- Ponce, V.M., Hawkins, E.R.H., 1996. Runoff curve number: has it reached maturity?. *J. Hydrol. Eng.* 1, 11–19. [https://doi.org/10.1061/\(ASCE\)1084-0699\(1996\)1:1\(11\)](https://doi.org/10.1061/(ASCE)1084-0699(1996)1:1(11)).
- Prochaska, A.B., Santi, P.M., Higgins, J.D., Cannon, S.H., 2008. A study of methods to estimate debris flow velocity. *Landslides* 5, 431–444. <https://doi.org/10.1007/s10346-008-0137-0>.
- Righini, M., Surian, N., Wohl, E., Marchi, L., Comiti, F., Amponsah, W., Borga, M., 2017. Geomorphic response to an extreme flood in two Mediterranean rivers (northeastern Sardinia, Italy): analysis of controlling factors. *Geomorphology* 290, 184–199. <https://doi.org/10.1016/j.geomorph.2017.04.014>.
- Rinaldi, M., Simoncini, C., Piégay, H., 2009. Scientific design strategy for promoting sustainable sediment management: the case of the Magra River (Central-Northern Italy). *River Res. Appl.* 25, 607–625.
- Rinaldi, M., Surian, N., Comiti, F., Bussetini, M., 2013. A method for the assessment and analysis of the hydromorphological condition of Italian streams: the Morphological Quality Index (MQI). *Geomorphology* 180–181, 96–108.
- Rinaldi, M., Surian, N., Comiti, F., Bussetini, M., 2015. A methodological framework for hydromorphological assessment, analysis and monitoring (IDRAIM) aimed at promoting integrated river management. *Geomorphology* 251, 122–136.
- Rinaldi, M., Amponsah, W., Benvenuti, M., Borga, M., Comiti, F., Lucia, A., Marchi, L., Nardi, L., Righini, M., Surian, N., 2016. An integrated approach for investigating geomorphic response to extreme events: methodological framework and application to the October 2011 flood in the Magra River catchment, Italy. *Earth Surf. Process. Landf.* 41, 835–846. <https://doi.org/10.1002/esp.3902>.
- Scheidl, C., McDardell, B.W., Rickenmann, D., 2015. Debris-flow velocities and super-elevation in a curved laboratory channel. *Can. Geotech. J.* 52, 305–317. <https://doi.org/10.1139/cgj-2014-0081>.
- Scorpio, V., Roskopf, C.M., 2016. Channel adjustments in a Mediterranean river over the last 150 years in the context of anthropic and natural controls. *Geomorphology* 275, 90–104. <https://doi.org/10.1016/j.geomorph.2016.09.017>.
- Sloan, J., Miller, J.R., Lancaster, N., 2001. Response and recovery of the Eel River, California, and its tributaries to floods in 1955, 1964 and 1997. *Geomorphology* 36, 129–154.
- Steeb, N., Rickenmann, D., Badoux, A., Rickli, C., Waldner, P., 2017. Large wood recruitment processes and transported volumes in Swiss mountain streams during the extreme flood of August 2005. *Geomorphology* 260, 112–127.
- Stoffel, M., Wyzga, B., Marston, R.A., 2016. Floods in mountain environments: a synthesis. *Geomorphology* 272, 1–9. <https://doi.org/10.1016/j.geomorph.2016.07.008>.
- Surian, N., Barban, M., Ziliani, L., Monegato, G., Bertoldi, W., Comiti, F., 2015. Vegetation turnover in a braided river: frequency and effectiveness of floods of different magnitude. *Earth Surf. Process. Landf.* 40, 542–558. <https://doi.org/10.1002/esp.3660>.
- Surian, N., Righini, M., Lucia, A., Nardi, L., Amponsah, W., Benvenuti, M., Borga, M., Cavalli, M., Comiti, F., Marchi, L., Rinaldi, M., Viero, A., 2016. Channel response to extreme floods: insights on controlling factors from six mountain rivers in northern Apennines, Italy. In: *Geomorphology, Floods in Mountain Environments*. vol. 272, pp. 78–91. <https://doi.org/10.1016/j.geomorph.2016.02.002>.
- Thompson, C., Croke, J., 2013. Geomorphic effects, flood power, and channel competence of a catastrophic flood in confined and unconfined reaches of the upper Lockyer valley, southeast Queensland, Australia. *Geomorphology* 197, 156–169.
- Toone, J., Rice, S.P., Piégay, H., 2012. Spatial discontinuity and temporal evolution of channel morphology along a mixed bedrock-alluvial river, upper Drôme River, southeast France: contingent responses to external and internal controls. *Geomorphology* <https://doi.org/10.1016/j.geomorph.2012.05.033>.
- Wohl, E.E., Greenbaum, N., Schick, A.P., Baker, V.R., 1994. Controls on bedrock channel incision along Nahal Paran, Israel. *Earth Surf. Process. Landf.* 19, 1–13.
- Wolman, M.G., Gerson, R., 1978. Relative scales of time and effectiveness of climate in watershed geomorphology. *Earth Surf. Process. Landf.* 3, 189–208.